POST HEAT TREATMENT OPTIMIZATION OF COLD SPRAY AM INCONEL 718

This study investigates the post HT conditions required to produce Inconel 718 parts via cold spray additive manufacturing that meet functional performance standards.

By APTULLAH KARAKAŞ, ARASH ATAEE, AMIT RATHI, TEVFIK OZAN FENERCIOĞLU, CAN ERDOGAN,AND TUNCAY YALÇINKAYA

The cold spray technique has recently emerged as an additive manufacturing method for producing free-standing parts in addition to its use in repair and coating applications. Manufacturing relatively hard alloys such as Inconel 718 remains challenging and requires careful optimization of process parameters and post-heat treatment (HT) conditions. This work investigates the optimal post-heat treatment procedure for cold-sprayed Inconel 718 parts, focusing on both temperature and duration of the heat-treatment process. Cold-sprayed parts are initially heat-treated at 968°C, 1,066°C, and 1,200°C for 1 hour, followed by a conventional aging procedure. Results indicate that heat treatment at 1,200°C reduces porosity and enhances ductility in tensile tests. Furthermore, to assess the effect of HT closer to the material's melting point, samples are heat-treated above 1,200°C. Further analysis of the HT temperatures reveals that heat treatment at 1,260°C yields the lowest porosity values and shows strong potential to meet manufacturing standards.

INTRODUCTION

Efficient ways to manufacture metallic structures with flexible topologies and sustainable processes have become a highly popular topic in recent years. Thermal spray technologies have advanced significantly, allowing for the deposition of materials and coatings with precise geometric and mechanical properties. Cold spray (CS) essentially exemplifies the extreme end of thermal spray techniques allowing material deposition at temperatures well below their melting points. Primarily emerging as a coating technique [1,2], CS deposition has gradually been recognized as an additive manufacturing and repairing technology owing to its unique capabilities [3,4,5,6]. CS can be regarded as a high-speed manufacturing process capable of producing free standing parts without size limitations, applicable to a wide range of materials, including aluminium [7,8] and titanium [9,10], nickel alloys [11,12] and compositions of different materials [13,14].

In CS process, a regulated driving gas is used as the main source of motion for powder to be accelerated and sprayed over a building plate. Compressed gas (typically nitrogen or helium) is heated and mixed with the powder that runs through a powder feeder. The mixture is delivered to a de Laval-type (convergent-divergent) nozzle to accelerate the mixture to supersonic speeds up to 1,200 m/s [15]. Particles are then sprayed onto a metal substrate using a robot arm to control the deposition speed and the geometry of the part. The deposition of material solely occurs due to the high-kinetic energy impact of particles, leading to plastic deformation and bonding between powder particles or particles and substrate [16,17,18].

The inherent advantage of the CS technique lies in its operational characteristic of low process temperatures. Despite the heating of the driving gas, CS additive manufacturing (CSAM) is conducted at temperatures lower than the melting point of the materials involved, ensuring the metal powder remains in a solid-state form. The nature of the process prevents detrimental structural changes, enabling the deposition of oxygen-sensitive materials with minimized thermal effects. Crystal structure and phase compositions can be preserved for a wide range of powder materials and shapes. CS process enables the fusion of dissimilar metals for engineering of multi-material parts with combinations of superior properties such as strength, corrosion, and wear resistance [19,20].

Such advantages make CS process an important manufacturing alternative for nickel-based alloys such as Inconel series — special nickel-based super alloys designed for high strength-high temperature applications and chemically aggressive environments such as gas turbines and nuclear reactors. It is an expensive material due to application specific properties and largely manufactured by a combination of special melting techniques, such as vacuum induction melting (VIM), and forging methods that are combined with precise heat treatment (HT) and machining operations. CS has gained attention as an alternative manufacturing technique for Inconel alloys in recent years [21,22,23]. The high-deposition efficiency, low porosity, and minimal thermal distortion achieved through the CS process demonstrate significant potential to prevent material waste from conventional machining operations and reduce carbon emissions.

Cold-sprayed parts in their as-sprayed condition are practically unusable due to quasi-brittle behavior and poor surface quality resulting from the severe plastic deformation-driven deposition process. This commonly necessitates post HT and surface finishing procedures [18] to ensure the parts meet functional requirements. Additionally, the process parameters need to be tailored to specific metal powder to achieve minimum porosity and maximum deposition efficiency. Critical particle velocity required to reach sufficient bonding is typically higher for Inconel or titanium alloys compared to softer materials such as copper or aluminum alloys. These factors further complicate the deposition process with CS for Inconel 718. Several factors contribute to reducing the porosity of cold-sprayed parts in their as-sprayed condition. The choice of driving gas significantly affects both the mechanical properties of parts in their as-sprayed and heat-treated states [24,25]. Nitrogen is commonly selected as the driving gas due to its cost-effectiveness, whereas CS with helium results in lower porosity parts at lower gas pressures, attributed to the increased kinetic energy of powder particles for Inconel 718 [26]. Additionally, microforging-assisted deposition [27], involves the addition of hard steel particles to the powder mix to further forge the Inconel particles and enhance plastic deformation. This method can reduce porosity by up to 0.17%. Nevertheless, post HT procedures are still necessary to restore ductility in these low-porosity samples.

Numerous studies have investigated the effects of post HT on cold-sprayed samples [28,29,30,31]. For cold-sprayed Inconel 718, post HT is typically performed at temperatures between 800°C and 1,200°C to enhance the metallurgical bonding and reduce porosity [21,23,26,27,32], though some studies have explored treatments at tem-

peratures exceeding 1,200°C [11,33]. HT at approximately 1,200°C for 1 hour has been reported to result in a significant increase in ductility with only a slight reduction in strength, while increasing the HT temperature to 1,250°C appears to reduce porosity further. Still, there is no solid consensus on the optimum HT conditions for cold-sprayed Inconel 718 to produce high-quality parts, especially for treatments at temperatures near the alloy's melting point, which remain underexplored. This study aims to address this gap by examining the effects of various post-HT conditions and aging process on the porosity, ductility, and hardness of cold-sprayed Inconel 718 samples. Samples are characterized in terms of microstructure, final porosity, ductility, and hardness values after different heat treatment and ageing procedures.

METHODOLOGY

Cold spray additive manufacturing

CS additive manufacturing (CSAM) processes are carried out with the TKF-9000 cold spray equipment manufactured by Titomic. CS is performed onto aluminum tubes with a diameter of 50 mm and length of 150 mm as shown in Figure 1. The final part diameter is 80 mm. The manufacturing strategy involves using a zig-zag toolpath, where the cylindrical part rotates while the CS robot traversed back and forth in a zigzag pattern, first from A to B, then from B to A, with A and B representing opposite ends of the part. A total of 80 passes are made to complete the sample. Inconel 718 powder is sourced from Tekna company. The average powder particle diameter is 17.86 µm, with a particle size distribution of D10 = 7.08 µm, D50 = 15.80 µm, and D90 = 36.18 µm. The SEM micrograph of the Inconel 718 powder is shown in Figure 1, illustrating that the particles exhibit high sphericity, with a notable presence of satellite particles measuring less than 3 µm in diameter. CS process parameters include:

- **Propelling gas:** Nitrogen (N_2).
- **Gas pressure:** 5 MPa.
- **Gas temperature:** 950°C.
- **Nozzle standoff distance:** 30 mm.
- **Carrier gas flow rate:** 200 SLM.
- **Stepover spacing:** 2 mm.
- **Surface speed:** 500 mm/sec.

Heat treatment and aging procedures

Post HT and aging processes are applied to the as-sprayed parts. Initially, Inconel 718 parts are subjected to heat treatment at temperatures of 968°C, 1,066°C, and 1,200°C for 2 hours in a muffle furnace, followed by cooling in open air. This process aims to enhance ductility, reduce porosity, and recrystallize grains from the dendritic structure. Subsequently, the parts undergo an aging procedure at 720°C for 8 hours, followed by furnace cooling to 620°C and held for another 8 hours. Finally, the parts are air-cooled to room temperature. The aging treatment follows the AMS 5663 standard. Furthermore, as-sprayed parts are heat-treated at a temperature closer to the melting point of the Inconel 718 alloy. Heat treatment is performed at 1,230°C, 1,260°C and 1,290°C for 2 and 4 hours to further decrease the porosity of the parts. No aging is applied to these samples. Tensile testing is not performed for these trials since these samples are too small for standard testing; thus, only porosity and hardness measurements are performed.

Microstructural characterization

The grain size and porosity measurements are carried out using optical images taken with a Olympus BX53M optical microscope from 20 different locations following ASTM E112-12 and ASTM E2109-01 standards. These measurements are then averaged and reported.

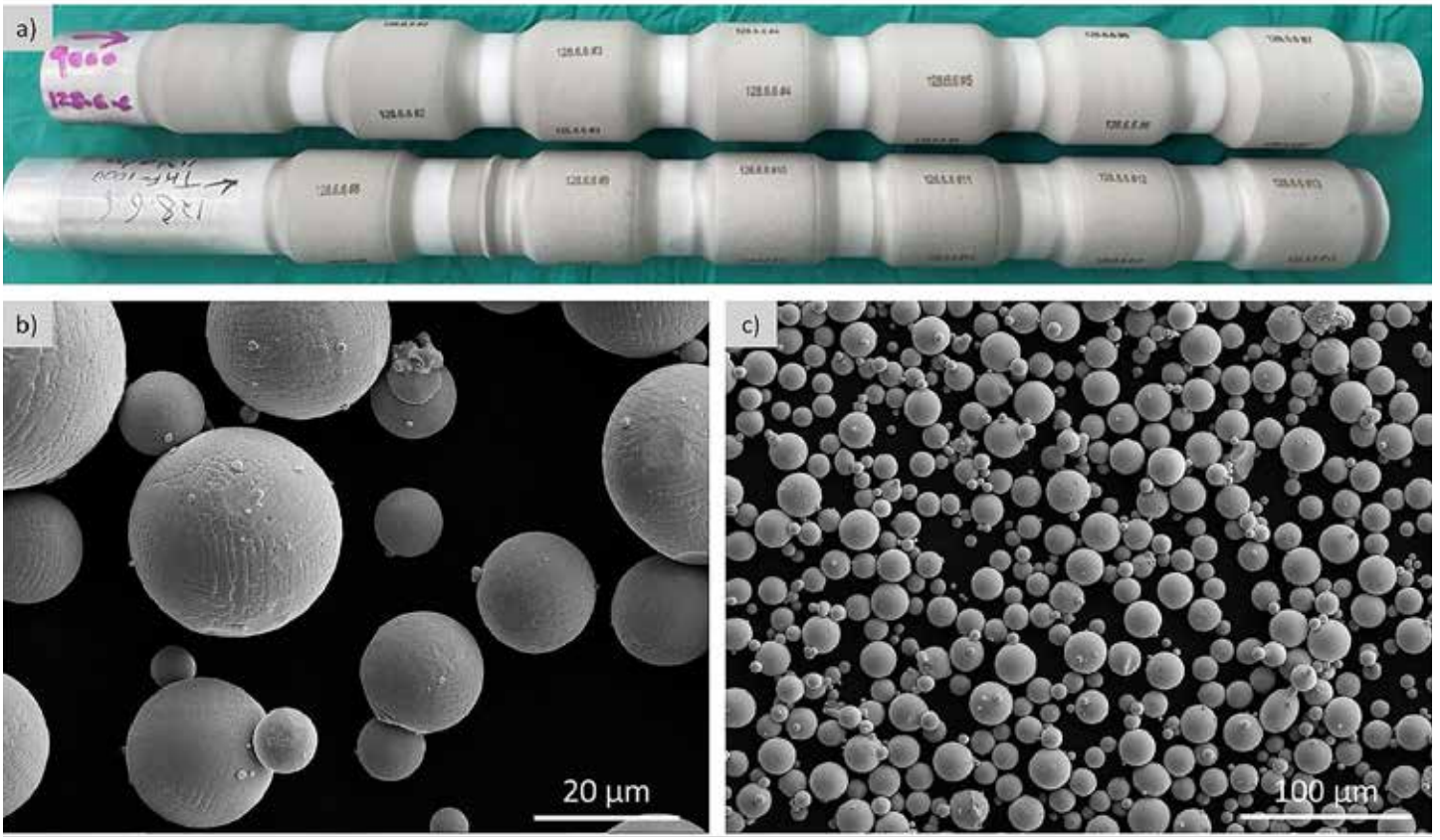

Figure 1: Cylindrical part with cold-sprayed Inconel 718 sections (a) SEM micrographs of the Inconel 718 powder under (b) 1,500x and (c) 250x magnification.

	As-sprayed	968°C	1066°C	1200°C
Porosity [%]	2.49	2.14	2.02	1.59

Table 1: Porosity values of samples subject to different HT conditions.

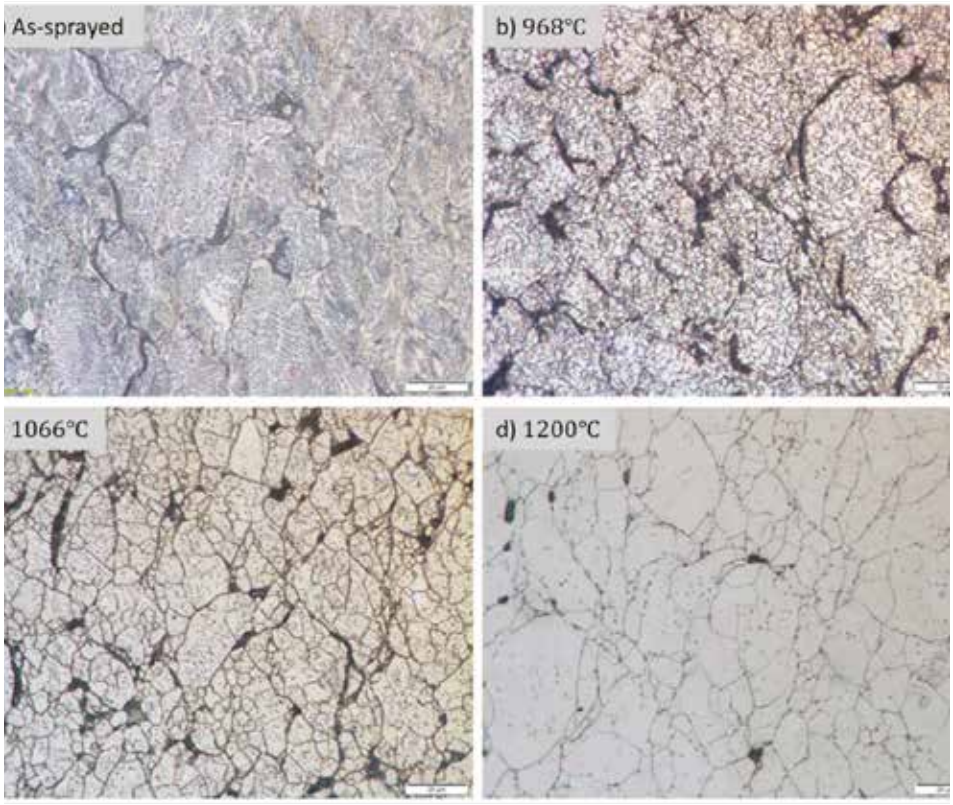

Figure 2: Optical microscope images of cold sprayed Inconel 718 samples in as-sprayed and different HT conditions.

For porosity measurement, voids are marked with a different color and porosity and calculated by an image analysis based on the area percentage of voids. Additionally, porosity uniformity in both the transverse and longitudinal directions relative to the cold spray gun scanning direction is checked, and no significant variations are observed, confirming the uniformity of porosity throughout the samples. Cold-sprayed Inconel 718 is further characterized for grain morphology and phase distributions. In order to evaluate and compare these characteristics in detail, a scanning electron microscopy (SEM) is conducted by a Thermo Fisher Scientific Quanta 650 field emission gun scanning electron microscope (FEG-SEM). Grain structure, secondary phases, and porosities are examined by SEM after etching with oxalic acid for 15 seconds.

Mechanical characterization

Heat-treated parts are sectioned with a coolant-assisted diamond wheel mounted in a phenolic resin, then ground and polished. Samples are cut using wire EDM (electrical discharge machining) from the sectioned cylindrical parts. Tensile tests are performed according to the ASTM E8/E8M-13 standard using an Instron 3382 universal testing machine at a constant speed of 5 mm/min. An extensometer over a gage length of 50 mm is used for all tensile tests. Hardness measurements are performed according to ASTM E384 standard using an EmcoTest DuraScan-20 testing machine with 200 g (HV 0,2) for 5 seconds.

Results and discussion

The microstructures of samples in as-sprayed condition and after HT at temperatures of 968°C, 1,066°C, and 1,200°C following CSAM are shown in Figure 2. In as-sprayed condition, samples exhibit a dendrite structure, a distinctive structure of crystals as metals solidifies, as shown in Figure 2. The dendrite structure is typically formed during the manufacturing of powder (e.g. [31,34]) and preserved after CS. The particle boundaries that form during the CS process are visible, indicating particles are not fully bonded and the parts show brittle behavior in this condition as demonstrated extensively in the literature. Additionally, voids typically remain in the triple junctions where multiple particles contact one another. The porosity is measured to be 2.49% in as-sprayed condition in agreement with the published data [11,30,33] for cold-sprayed Inconel 718. Significant reduction in porosity and further bonding of the material is achieved with the HT process. During the HT process, solid-state diffusion occurs between the particles, similar to the sintering mechanism. This diffusion facilitates the transformation of the dendritic structure into newly recrystallized grains, which effectively reduces the porosity. The porosity is reduced up to 1.59% as shown in Table 1 with HT at 1,200°C. Recrystallization occurs after HT at all three temperatures, with new grain sizes observed to be at 1-2µm after 968°C, 5-10µm after 1,066°C and 15-20µm after 1,200°C.

The results of tensile testing for the heat-treated samples are illustrated in Figure 3. It is clear from the data that the ductility of the samples increased proportionally with the rise in heat-treatment temperature peaking at about 16%, accompanied by a decrease in yield stress. However, despite these variations, the ultimate strength of the components remains relatively consistent, typically hovering around 800 MPa. In Figure 3, test results after aging treatment is demonstrated. Experiments are repeated three times for each HT. All specimens reached a similar level of yield stress and hardening capacity, with those heat-treated at 968°C being the least strong and ductile. The level of porosity before the aging treatment has a direct impact on ductility, with specimens heat-treated at 1,200°C achieving the highest ductility, exhibiting 8% elongation at fracture.

Hardness measurement results are depicted in Figure 4 through the thickness of the CS deposit. Values are found to be between 450-550 HV for CS sample in as-sprayed condition. After HT, hardness reduced below 350 HV except at the outer surface. As the HT temperature increased, the hardness values are further decreased with more homogeneous distribution through the thickness, indicating an inhomogeneous microstructure of the material in as-sprayed state. After the aging treatment, hardness of the samples reached about 450 HV for all three HT temperatures.

A further analysis of microstructure, phases, and their distribution are conducted by SEM for the heat treated at 1,200°C and aged sample. Figure 5 shows micrographs at 20K and 60K magnifications. Gamma prime (γ') precipitates are formed in the grain interiors and delta phases are formed at the grain boundaries after the aging process. Similar precipitate morphology can be observed with Inconel 718 alloy produced by conventional methods. Furthermore, gamma

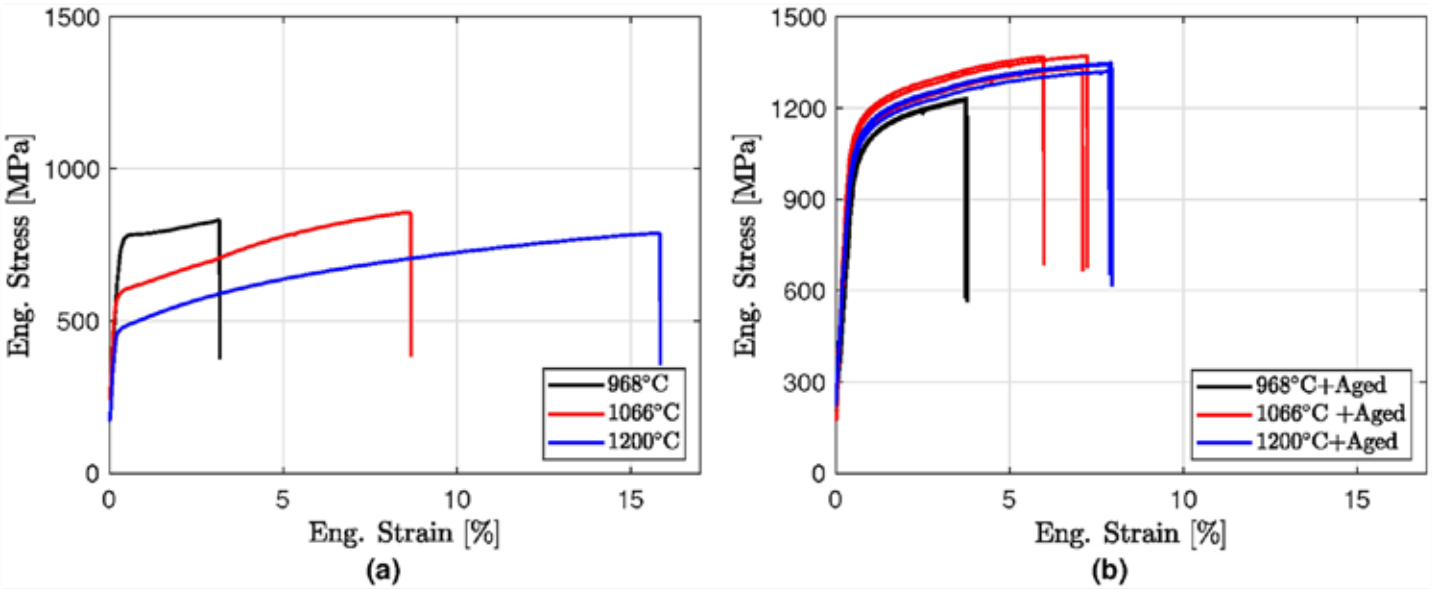

Figure 3: Engineering stress vs. strain response of the heat-treated cold-sprayed samples (a) before and (b) after aging.

double prime (γ'') precipitates with plate-like structures and 60-70 nm in size are formed. A not fully bonded interface can be observed in the SEM image as well.

Heat treatments at temperatures exceeding 1,200°C is performed, with the results presented in Table 2. For HT at 1,290°C, only the 2-hour results are available, as equipment limitations prevented completion of the 4-hour treatment. A notable decrease in porosity is observed with increasing temperatures compared to the 1,200°C treatment, achieving a minimum porosity of 0.25% at 1,260°C after 2 hours. Extending the treatment duration from 2 to 4 hours does not yield significant changes in porosity or hardness. Additionally, no further reduction in porosity is observed at 1,290°C compared to the results at 1,260°C. The hardness of samples HT at 1,230°C and 1,260°C is comparable to those HT at 1,200°C, while a greater variation in hardness is observed at 1,290°C, potentially due to partial melting of the material.

Figure 6 compares the strength and ductility outcomes of cold-sprayed Inconel 718 samples from current research with results available in the literature. The data from this work focuses on the sample heat-treated at 1,200°C, both before and after the aging procedure. Notably, this sample shows the highest strength among all compared examples, with a significant amount of elongation prior to fracture. Furthermore, to the best of the authors' knowledge, this study is the first to report tensile testing results for conventionally aged cold-sprayed Inconel 718. Two literature examples [26,27] represent furnace-cooled samples, which exhibit a microstructural change and small σ precipitates to form resembling a short aging process27. It is important to note the process parameters and heat treatment (HT) conditions vary noticeably among the samples in Figure 6. An outlier in ductility is observed for a sample heat-treated at 1250°C for 1 hour [11], highlighting the potential for optimizing HT conditions to significantly enhance the mechanical properties of cold-sprayed Inconel 718 parts. This agrees with the current findings and emphasizes the opportunity for further improvement

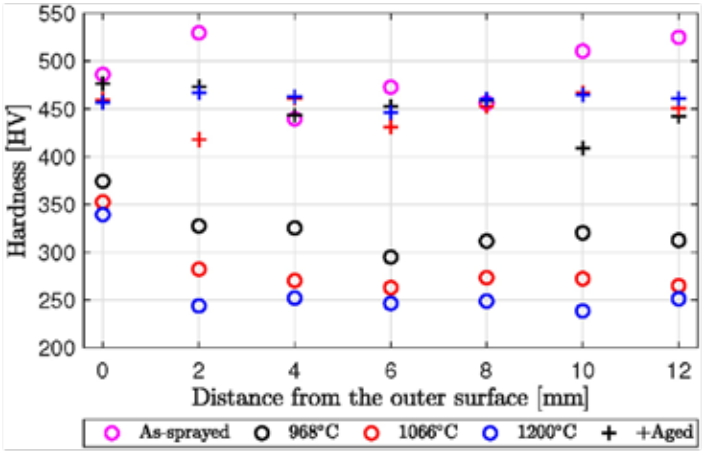

Figure 4: Hardness values through the thickness of the cold-sprayed parts.

in both ductility and strength through precise fine-tuning of HT parameters.

CONCLUDING REMARKS

This study investigates the post HT conditions required to produce Inconel 718 parts via cold spray additive manufacturing that meet functional performance standards. Selecting optimal post-HT conditions is essential to achieving cold-sprayed parts with practical properties. In the as-sprayed state, parts exhibit a dendritic microstructure with visible particle boundaries. Post-HT processing leads to recrystallization of the crystal structure, significant porosity reduction, and enhanced metallurgical bonding. Samples heat-treated at 1,200°C and subsequently aged demonstrate the highest strength value compared to those reported in the literature with considerable amount of ductility (8%). Analysis of HT conditions above 1,200°C reveals that porosity as low as 0.25% can be achieved, with 1,260°C for 2 hours identified as the optimal HT condition. These findings

Temp. (°C)	Duration (h)	Porosity (%)	Hardness (HV)	Duration (h)	Porosity (%)	Hardness (HV)
1230	2	0.62	250-270	4	0.70	250-270
1260	2	0.25	220-250	4	0.30	220-250
1290	2	0.29	210-360	-	-	-

Table 2: Porosity and hardness levels for heat treated samples at 1,230°C, 1,260°C, and 1,290°C for 2- and 4-hour durations.

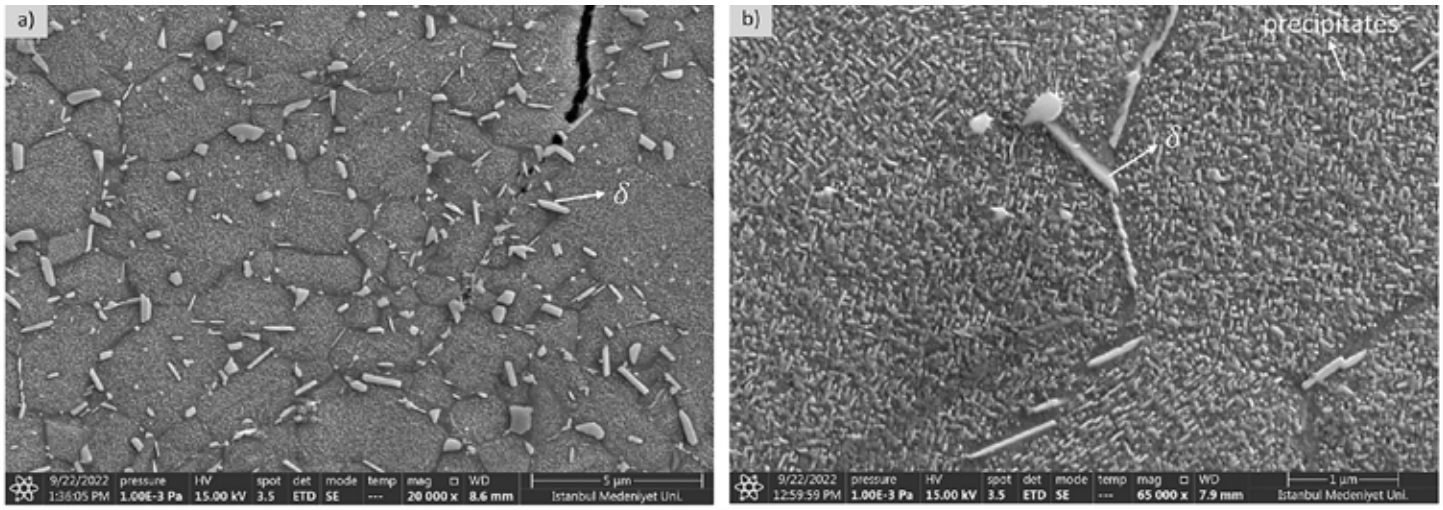

Figure 5: SEM images of cold-sprayed Inconel 718 samples at (a) 20,000x and (b) 65,000x magnification.

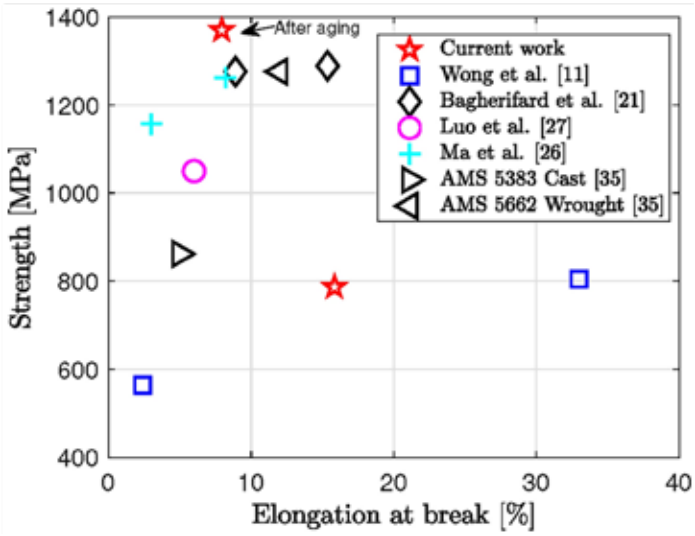

Figure 6: Strength and ductility results for the cold sprayed Inconel 718 samples. AMS5383 and AMS5662 data [35].

indicate that CSAM Inconel 718 parts treated under these conditions have the potential to closely match the mechanical properties of conventionally manufactured counterparts while preserving the unique advantages of additive manufacturing.

DATA AVAILABILITY

All data generated or analyzed during this study are included in this published article.

CONTRIBUTIONS

A.K: conceptualization, methodology, visualization, writing original draft, review and editing. A.A: conceptualization, methodology, visualization, writing original draft, review and editing. A.R: conceptualization, methodology, visualization, writing original draft, review and editing. T.O.F: conceptualization, methodology, visualization, writing original draft, review and editing, funding acquisition. C.E.: conceptualization, methodology, visualization, writing original draft, review and editing. T.Y.: conceptualization, methodology, supervision, writing original draft, review and editing.

COMPETING INTERESTS

The authors declare no competing interests.

PUBLISHER'S NOTE

Springer Nature remains neutral with regard to jurisdictional claims in published maps and institutional affiliations.

REFERENCES

[1] Gärtner, F. et al. Mechanical properties of cold-sprayed and thermally sprayed copper coatings. Surface and Coatings Technology 200, 6770–6782. https://doi.org/10.1016/j.surfcoat.2005.10.007 (2006).

[2] Ghelichi, R. & Guagliano, M. Coating by the cold spray process: A state of the art. Frattura ed Integrità Strutturale 3, 30–44. https://doi.org/10.3221/IGF-ESIS.08.03 (2013).

[3] Blose, R., Walker, B., Walker, R. & Froes, S. New opportunities to use cold spray process for applying additive features to titanium alloys. Metal Powder Report 61, 30–37. https://doi.org/10.1016/S0026-0657(06)70713-5 (2006).

[4] Cadney, S., Brochu, M., Richer, P. & Jodoin, B. Cold gas dynamic spraying as a method for freeforming and joining materials. Surface and Coatings Technology 202, 2801–2806. https://doi.org/10.1016/j.surfcoat.2007.10.010 (2008).

[5] Yin, S., Hassani, M., Xie, Q. & Lupoi, R. Unravelling the deposition mechanism of brittle particles in metal matrix composites fabricated via cold spray additive manufacturing. Scripta Materialia 194, 113614. https://doi.org/10.1016/j.scriptamat.2020.10.055 (2021).

[6] Zhang, Z. L., Afrasiabi, M. & Bambach, M. A meshless computational framework for studying cold spray additive manufacturing including large numbers of powder particles with diverse characteristics. Scientific Reports 14, 11393. https://doi.org/10.1038/s41598-024-62091-2 (2024).

[7] Morgan, R., Fox, P., Pattison, J., Sutcliffe, C. & O'Neill, W. Analysis of cold gas dynamically sprayed aluminium deposits. Materials Letters 58, 1317–1320. https://doi.org/10.1016/j.matlet.2003.09.048 (2004).

[8] Weiller, S. & Delloro, F. A numerical study of pore formation mechanisms in aluminium cold spray coatings. Additive Manufacturing 60, 103193. https://doi.org/10.1016/j.addma.2022.103193 (2022).

[9] Li, C.-J. & Li, W.-Y. Deposition characteristics of titanium coating in cold spraying. Surface and Coatings Technology 167, 278–283. https://doi.org/10.1016/S0257-8972(02)00919-2 (2003).

[10] Li, W., Cao, C. & Yin, S. Solid-state cold spraying of Ti and its alloys: A literature review. Progress in Materials Science 110, 100633. https://doi.org/10.1016/j.pmatsci.2019.100633 (2020).

[11] Wong, W. et al. Cold spray forming of Inconel 718. Journal of Thermal Spray Technology 22, 413–421. https://doi.org/10.1007/s11666-012-9827-1 (2013).

[12] Chaudhuri, A., Raghupathy, Y., Srinivasan, D., Suwas, S. & Srivastava, C. Microstructural evolution of cold-sprayed Inconel 625 superalloy coatings on low alloy steel substrate. Acta Materialia 129, 11–25. https://doi.org/10.1016/j.actamat.2017.02.070 (2017).

[13] Heydari Astaraee, A., Colombo, C. & Bagherifard, S. Insights on metallic particle bonding to thermoplastic polymeric substrates during cold spray. Scientific Reports 12, 18123. https://doi.org/10.1038/s41598-022-22200-5 (2022).

[14] Wang, Z. et al. Deposition mechanism of ceramic reinforced metal matrix composites via cold spraying. Additive Manufacturing 85, 104167. https://doi.org/10.1016/j.addma.2024.104167 (2024).

[15] Yin, S., Meyer, M., Li, W., Liao, H. & Lupoi, R. Gas flow, particle acceleration, and heat transfer in cold spray: A review. Journal of Thermal Spray Technology 25, 874–896. https://doi.org/10.1007/s11666-016-0406-8 (2016).

[16] Assadi, H., Kreye, H., Gärtner, F. & Klassen, T. Cold spraying - A materials perspective. Acta Materialia 116, 382–407. https://doi.org/10.1016/j.actamat.2016.06.034 (2016).

[17] Rokni, M. R., Nutt, S. R., Widener, C. A., Champagne, V. K. & Hrabe, R. H. Review of relationship between particle deformation, coating microstructure, and properties in high-pressure cold spray. Journal of Thermal Spray Technology 26, 1308–1355. https://doi.org/10.1007/s11666-017-0575-0 (2017).

[18] Yin, S. et al. Cold spray additive manufacturing and repair: Fundamentals and applications. Additive Manufacturing 21, 628–650. https://doi.org/10.1016/j.addma.2018.04.017 (2018).

[19] Yu, M., Suo, X., Li, W., Wang, Y. & Liao, H. Microstructure, mechanical property and wear performance of cold sprayed Al5056/SiCp composite coatings: Effect of reinforcement content. Applied Surface Science 289, 188–196. https://doi.org/10.1016/j.apsusc.2013.10.132 (2014).

[20] Yu, M., Chen, H., Li, W.-Y., Suo, X. K. & Liao, H. L. Building-up process of cold-sprayed Al5056/In718 composite coating. Journal of Thermal Spray Technology 24, 579–586. https://doi.org/10.1007/s11666-014-0205-z (2015).

[21] Bagherifard, S. et al. Cold spray deposition for additive manufacturing of freeform structural components compared to selective laser melting. Materials Science and Engineering: A 721, 339–350. https://doi.org/10.1016/j.msea.2018.02.094 (2018).

[22] Zhang, Z. et al. Cold spray deposition of Inconel 718 in comparison with atmospheric plasma spray deposition. Applied Surface Science 535, 147704. https://doi.org/10.1016/j.apsusc.2020.147704 (2021).

[23] Shrestha, D., Azarmi, F. & Tangpong, X. W. Effect of heat treatment on residual stress of cold sprayed nickel-based superalloys. Journal of Thermal Spray Technology 31, 197–205. https://doi.org/10.1007/s11666-021-01284-x (2022).

[24] Ozdemir, O. C., Widener, C. A., Helfritch, D. & Delfanian, F. Estimating the effect of helium and nitrogen mixing on deposition efficiency in cold spray. Journal of Thermal Spray Technology 25, 660–671. https://doi.org/10.1007/s11666-016-0394-8 (2016).

[25] MacDonald, D., Rahmati, S., Jodoin, B. & Birtch, W. An economical approach to cold spray using in-line nitrogen-helium blending. Journal of Thermal Spray Technology 28, 161–173. https://doi.org/10.1007/s11666-018-0813-0 (2019).

[26] Ma, W. et al. Microstructural and mechanical properties of high-performance Inconel 718 alloy by cold spraying. Journal of Alloys and Compounds 792, 456–467. https://doi.org/10.1016/j.jallcom.2019.04.045 (2019).

[27] Luo, X.-T., Yao, M.-L., Ma, N., Takahashi, M. & Li, C.-J. Deposition behavior, microstructure and mechanical properties of an in-situ micro-forging assisted cold spray enabled additively manufactured Inconel 718 alloy. Materials & Design 155, 384–395. https://doi.org/10.1016/j.matdes.2018.06.024 (2018).

[28] Huang, R., Sone, M., Ma, W. & Fukanuma, H. The effects of heat treatment on the mechanical properties of cold-sprayed coatings. Surface and Coatings Technology 261, 278–288. https://doi.org/10.1016/j.surfcoat.2014.11.017 (2015).

[29] Rokni, M., Widener, C., Champagne, V., Crawford, G. & Nutt, S. The effects of heat treatment on 7075 Al cold spray deposits. Surface and Coatings Technology 310, 278–285. https://doi.org/10.1016/j.surfcoat.2016.10.064 (2017).

[30] Sun, W. et al. Improving microstructural and mechanical characteristics of cold-sprayed Inconel 718 deposits via local induction heat treatment. Journal of Alloys and Compounds 797, 1268–1279. https://doi.org/10.1016/j.jallcom.2019.05.099 (2019).

[31] Pérez-Andrade, L. et al. Optimization of Inconel 718 thick deposits by cold spray processing and annealing. Surface and Coatings Technology 378, 124997. https://doi.org/10.1016/j.surfcoat.2019.124997 (2019).

[32] Bagherifard, S. et al. Cold spray deposition of freestanding inconel samples and comparative analysis with selective laser melting. Journal of Thermal Spray Technology 26, 1517–1526. https://doi.org/10.1007/s11666-017-0572-3 (2017).

[33] Levasseur, D., Yue, S. & Brochu, M. Pressureless sintering of cold sprayed Inconel 718 deposit. Materials Science and Engineering: A 556, 343–350. https://doi.org/10.1016/j.msea.2012.06.097 (2012).

[34] Hajmrle, K., Angers, R. & Dufour, G. Phase analysis of sintered and heat treated alloy 718. Metallurgical Transactions A 13, 5–12. https://doi.org/10.1007/BF02642410 (1982).

[35] Zhang, D., Niu, W., Cao, X. & Liu, Z. Effect of standard heat treatment on the microstructure and mechanical properties of selective laser melting manufactured Inconel 718 superalloy. Materials Science and Engineering: A 644, 32-–40. https://doi.org/10.1016/j.msea.2015.06.021 (2015).

ABOUT THE AUTHOR

Aptullah Karakaş & Tevfik Ozan Fenercioğlu are with Repkon Machine and Tool Industry and Trade Inc. Arash Ataee & Amit Rathi are with Titomic Ltd. Can Erdogan and Tuncay Yalçinkaya are with Department of Aerospace Engineering, Middle East Technical University.